Geophysical Research Letters

RESEARCH LETTER
10.1029/2018GL081837

Discrepancy in the Identification of the Atlantic/Pacific Front in the Central Arctic Ocean: NO Versus Nutrient Relationships

Matthew B. Alkire[1], **Robert Rember**[2], **and Igor Polyakov**[2]

[1]Polar Science Center, Applied Physics Laboratory, University of Washington, Seattle, WA, USA, [2]International Arctic Research Center, University of Alaska Fairbanks, Fairbanks, AK, USA

Key Points:
- The NO parameter was used to separate upper halocline waters originating on the Chukchi versus East Siberian Sea shelves
- Traditional methods of identifying and separating Pacific from Atlantic waters in the central Arctic may no longer be reliable
- Pacific water was generally restricted to the Canadian Basin side of the Mendeleyev Ridge during summer 2015

Supporting Information:
- Supporting Information S1

Correspondence to:
M. B. Alkire,
malkire@apl.washington.edu

Citation:
Alkire, M. B., Rember, R., & Polyakov, I. (2019). Discrepancy in the identification of the Atlantic/Pacific front in the central Arctic Ocean: NO versus nutrient relationships. *Geophysical Research Letters*, *46*, 3843–3852. https://doi.org/10.1029/2018GL081837

Received 11 JAN 2019
Accepted 18 MAR 2019
Accepted article online 21 MAR 2019
Published online 1 APR 2019

Abstract Fronts in the NO parameter, a semiconservative tracer combining nitrate and dissolved oxygen, and dynamic height were observed in the central East Siberian Sea that distinguished Atlantic and Pacific contributions to the upper halocline of the Amerasian Basin during the summer of 2015. The NO front was aligned with the Transpolar Drift, and its position over the Mendeleyev Ridge indicates that Pacific waters were generally restricted to the Canada Basin and did not spread to the central Arctic. This interpretation lies in contrast to the distribution of Pacific water fractions, calculated using established relationships between nitrate and phosphate, and indicates that traditional tracers used to quantify Pacific water contributions to the Arctic Ocean are no longer accurate.

1. Introduction

The upper (0–450 m) water column of the Arctic Ocean generally consists of three layers: a cold and relatively fresh surface mixed layer, a halocline layer of increasing salinity with increasing depth, and a warm and saline Atlantic layer typically residing below 150 m. The halocline layer of the Arctic Ocean acts as a barrier separating Atlantic water heat from the surface and overlying sea ice; weakening and/or shoaling of the halocline will accelerate the loss of sea ice (Aagaard et al., 1981; Polyakov et al., 2017; Rudels et al., 1996; Steele & Boyd, 1998) but may also increase primary production via a release from nutrient limitation in certain areas (Ardyna et al., 2014; Nishino et al., 2008, 2013).

The halocline is ventilated from numerous sources, but most studies split it into two layers. The lower halocline is derived from Atlantic-origin waters and can be formed via freshening, cooling, and mixing of Atlantic waters in the Eurasian Basin or the Barents Sea, with additional influences from the Kara, Laptev, and/or East Siberian Seas (Alkire et al., 2017; Itoh et al., 2007; Rudels et al., 2004). In the Pacific sector of the Arctic Ocean (nominally the Chukchi Sea, Canada Basin, and part of the Makarov Basin), the lower halocline is overlain by upper halocline water (UHW) that is primarily derived from Pacific waters entering the Arctic via Bering Strait (Coachman & Barnes, 1961; Jones & Anderson, 1986; Shimada et al., 2005).

Identifying the presence or absence of Pacific water in the central Arctic (Alkire et al., 2007, 2015; Morison et al., 2006) and Fram Strait (Dodd et al., 2012; Falck et al., 2005; Taylor et al., 2003) provides clues regarding variations and/or trends in the upper (0- to 150-m depth) water circulation since the position of the front separating Atlantic and Pacific waters has been argued to correspond with the rough alignment of the Transpolar Drift (TPD) that moves water and sea ice from the Siberian shelves across the Arctic to Fram Strait (e.g., Morison et al., 1998, 2012). For example, when the TPD is aligned over the Lomonosov Ridge, the Pacific water influence is more widespread and contributes to the export through Fram Strait. However, if the TPD is shifted counterclockwise toward the Mendeleyev Ridge, the Pacific water influence is restricted (and export is typically restricted to the Canadian Archipelago) and warmer Atlantic waters spread farther into the Arctic interior (McLaughlin et al., 1996; Morison et al., 1998, 2000, 2002, 2006, 2012; Steele et al., 2004).

Pacific waters have typically been distinguished in the Arctic Ocean via high silicate (Jones & Anderson, 1986) and excess phosphate (PO_4^{3-}), relative to nitrate (NO_3^-), concentrations (Jones et al., 1998) that result from their interaction with Bering and Chukchi Sea sediments subject to intense organic matter (OM) remineralization and denitrification (Cooper et al., 1997; Jones & Anderson, 1986; Shimada et al., 2001, 2005).

However, denitrification has also been found to occur on the shelves of the East Siberian and Laptev Seas (Nitishinsky et al., 2007), complicating the identification of Pacific waters and their distribution in the Arctic Ocean (Bauch et al., 2011). Such complications are becoming more tenuous as the reduction in the sea ice cover over the East Siberian Sea (ESS) has facilitated the production of waters suitable to ventilate the upper halocline of the deep basins (Anderson et al., 2013, 2017; Nishino et al., 2013). These waters are geochemically similar to Pacific waters as they are characterized by high nutrient concentrations, low dissolved oxygen (O_2) concentrations, and low pH (Anderson et al., 2013).

These changing conditions in the Arctic Ocean have made it difficult to identify Pacific water influences using NO_3^-:PO_4^{3-} relationships and silicic acid concentrations. Alternative methods are needed if variations in the Atlantic/Pacific frontal position are to be accurately determined. In this study, we argue that the NO parameter might provide a suitable substitute for the qualitative identification of this front in the Arctic Ocean as NO_3^- and O_2 concentrations are typically higher in the Chukchi Sea compared to the ESS.

2. Data and Methods

Data are combined from various expeditions conducted in the Arctic during spring and summer of 2015, including the Nansen and Amundsen Basin Observation System II (NABOS-II) program, GEOTRACES, Beaufort Gyre Exploration Program (BGEP), North Pole Environmental Observatory (NPEO), and TransArc II (PS94) programs (Figure 1), as well as the 2008 expeditions of the International Siberian Shelf Study-08 (ISSS-08; Anderson et al., 2013) and *R/V Mirai* (Nishino et al., 2013). Specific details of the collection and analysis of NABOS-II data are provided in Text S1 of the supporting information. Operational details of the other expeditions are available on the corresponding project websites provided in Table S1 of the supporting information.

In order to ensure that the data sets were comparable, particularly in the ESS and Makarov Basin, O_2 and NO_3^- concentrations measured along NABOS-II transects ~165°E (section 4 in Figure 1) and ~175°E (section 5 in Figure 1) between depths of 500 and 1,000 m were compared against similar measurements made in the Makarov Basin during the 2015 GEOTRACES expedition, ISSS-08, and *Mirai* 2008 cruises (see Figures S1 and S2 and Table S2 of the supporting information). The depths were chosen as the O_2 and NO_3^- concentrations in deeper waters are expected to vary much less on larger spatial and temporal scales within the same general region (i.e., Makarov Basin). The mean O_2 and NO_3^- concentrations agreed well among these independent expeditions.

Measurements of O_2 and NO_3^- were combined to compute the NO parameter, a semiconservative parameter used to trace water masses at depths below the active layer of mixing and defined as $NO = (9 \times NO_3^-) + O_2$ (Broecker, 1974).

Pacific water fractions were calculated using NO_3^- and PO_4^{3-} concentrations according to the methods outlined in Yamamoto-Kawai et al. (2008). Dissolved inorganic nitrogen ($DIN = NO_3^- + NO_2^- + NH_4^+$) did not incorporate NH_4^+ concentrations as measurements were not available in all data sets. Pacific water fractions were not calculated using the NABOS-II data as it was determined that the PO_4^{3-} concentrations were questionable (see Text S1). Specific details regarding the Pacific water fraction calculations are provided in Text S2.

3. Results

The distributions of potential temperature (θ), dissolved oxygen (O_2), silicate, Pacific water fraction, NO_3^-, and NO for the West and East Legs of the GEOTRACES expedition are given in Figure 2. Although there were differences in the physical and geochemical distributions between these two legs, the general patterns were similar. We focus specifically on the upper halocline layer ($32 \leq S \leq 33.5$), marked by colder potential temperatures ($\theta < -1$°C; Figures 2a and 2b), moderate to low O_2 concentrations (<350 mmol/m^3; Figures 2c and 2d), higher silicate concentrations (>20 mmol/m^3; Figures 2k and 2l), and Pacific water fractions of ≥80% (Figures 2i and 2j).

These UHWs descended to depths of 250–300 m between ~73 and ~77°N and subsequently shoaled to ~100-m depth between 84 and 85°N. The θ, silicate, and Pacific water distributions all followed this pattern.

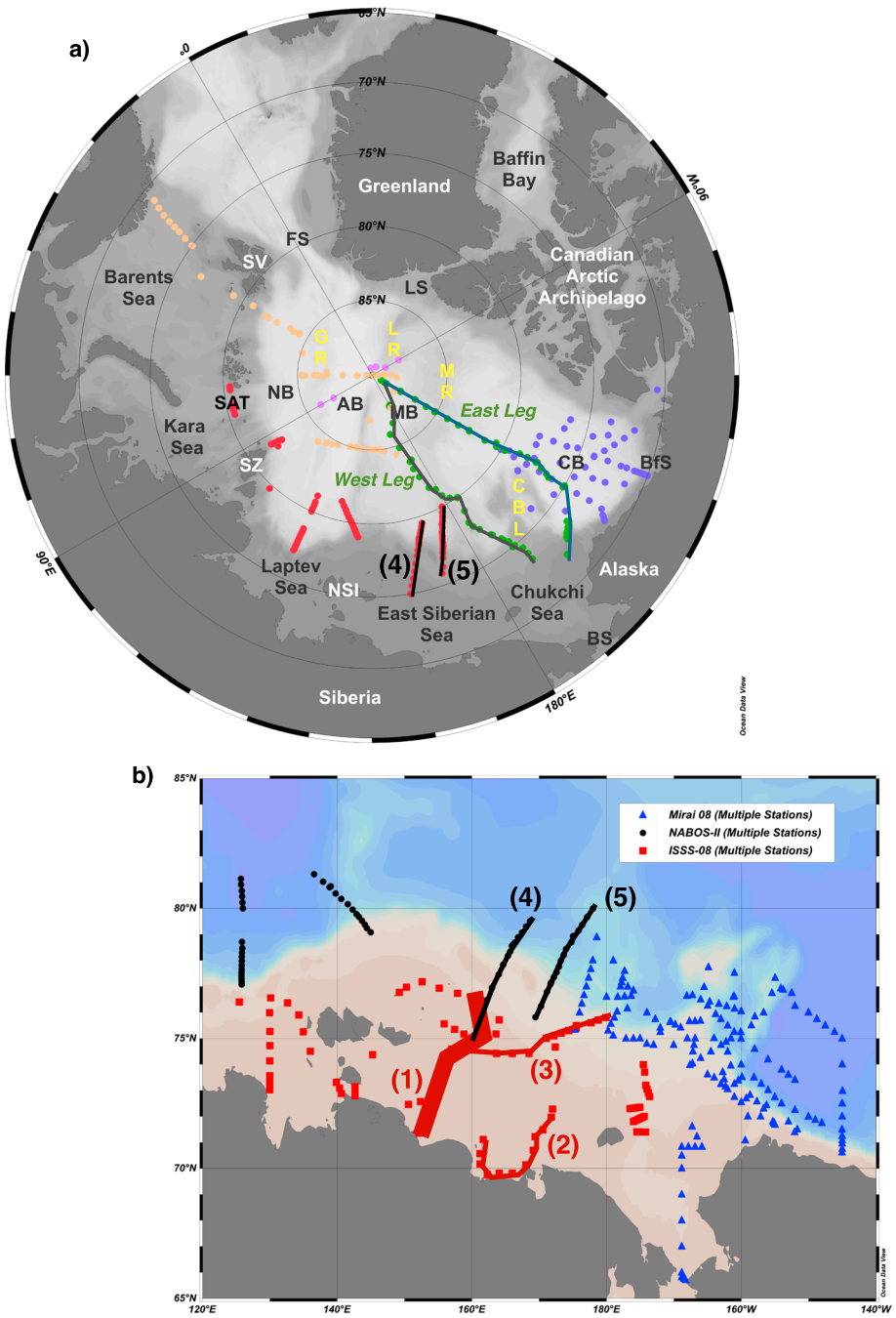

Figure 1. (a) Map of stations occupied during 2015 expeditions of North Pole Environmental Observatory (NPEO; purple dots), Nansen and Amundsen Basin Observation System II (NABOS-II; red dots), Beaufort Gyre Exploration Program (BGEP; blue dots), GEOTRACES (green dots), and PS94 (orange dots). Data from the West and East Legs of the GEOTRACES expedition (green lines) are presented in Figures 2 and S7. Data from NABOS-II sections 4 and 5 (black lines) are presented in Figures 4d–4g and S6. Relevant landmasses are listed in white, marginal seas and deep basins in black, and bathymetric features in yellow. BfS, Beaufort Sea; LS, Lincoln Sea; NB, Nansen Basin; AB, Amundsen Basin; MB, Makarov Basin; CB, Canada Basin; BS, Bering Strait; FS, Fram Strait; SV, Svalbard; SZ, Severnaya Zemlya; SAT, St. Anna trough; and NSI, New Siberian Islands. (b) Map of stations occupied during 2008 expeditions: *Mirai* (blue triangles) and International Siberian Shelf Study-08 (ISSS-08; red squares). Stations (and associated sections) occupied during the 2015 NABOS-II expedition are also shown as black dots (and lines), for comparison. Data from ISSS-08 sections 1–3 (red lines) are presented in Figures 4a–4c, S4, and S5. Maps created using Ocean Data View Software (Schlitzer, 2006).

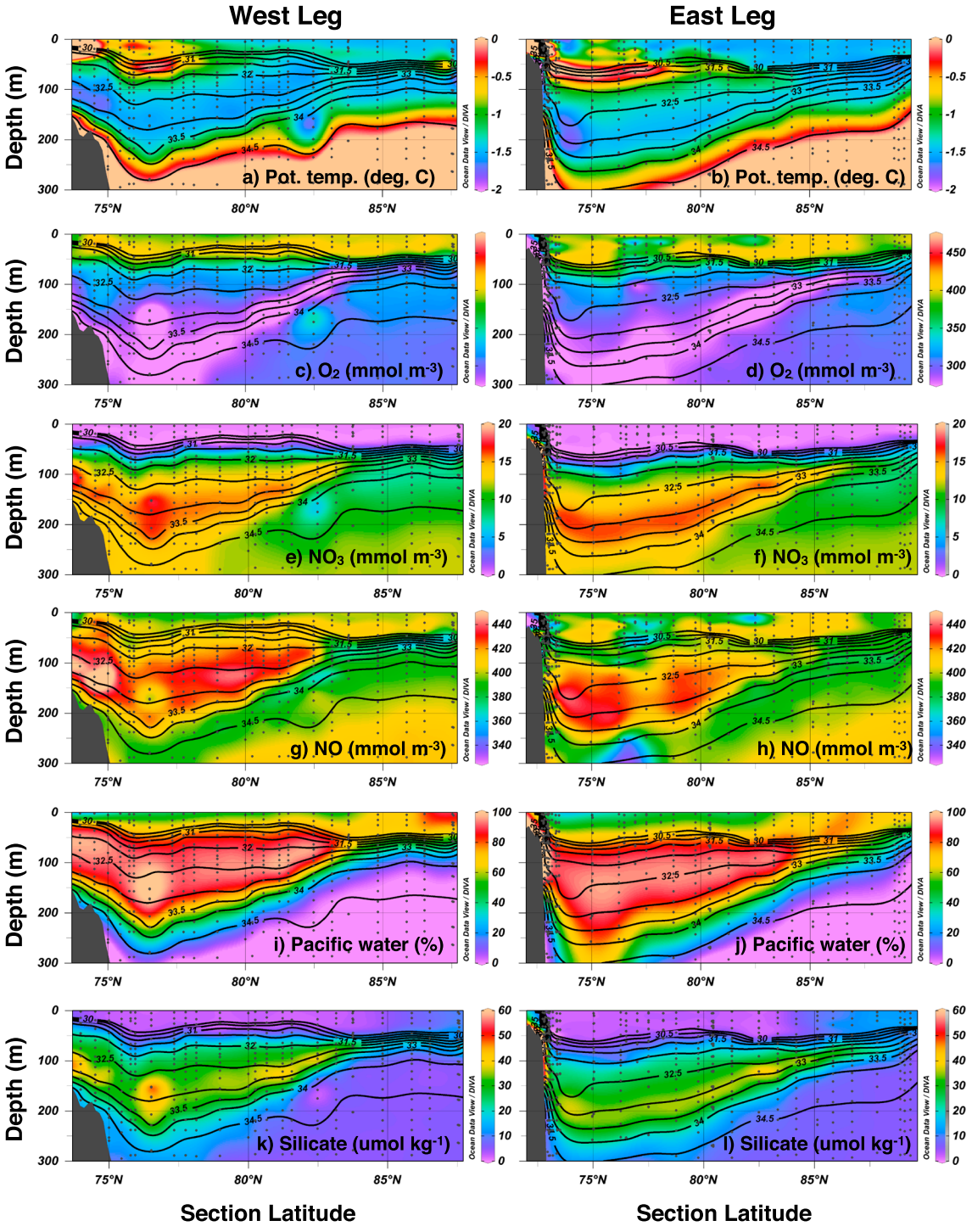

Figure 2. Sections of potential temperature, dissolved oxygen (O_2), nitrate (NO_3), NO, Pacific water fraction, and silicate along the west (left panels) and east (right panels) legs of the 2015 GEOTRACES expedition (see Figure 1 for section locations). Panels created using Ocean Data View Software (Schlitzer, 2006). Bottom topography from IBCAO (version 3) 90- × 30-s bathymetry.

However, the distribution of O_2 and NO (Figures 2g and 2h) were somewhat different. For example, the extent of the relatively high NO values (≥420 mmol/m^3) ended just north of ~82°N, whereas Pacific water fractions ≥40% and silicate concentrations ≥20 mmol/m^3 extended through the end of each leg. In addition, the O_2 minimum (<300 mmol/m^3) shoaled more steeply and to a shallower depth (~70 m) compared to the Pacific water or silicate distributions.

By combining the data sets collected by the various projects and programs operating in the Arctic during 2015, the differences observed between NO and the other geochemical parameters in Figure 2 were placed into a larger spatial context. The Pacific water fractions, silicate concentrations, and NO values corresponding to the S = 33 isohaline surface are plotted in Figure 3. In addition, Figure 3d shows the dynamic height (DH) at 100 m (relative to a prescribed level of no motion at 250 m), the approximate depth of the S = 33 isohaline at the northern ends of the GEOTRACES transects.

Relatively high Pacific water fractions (>60%) extended northward from the Chukchi Sea and Canada Basin into the Makarov Basin at latitudes >85°N (Figure 3a). Silicate concentrations exceeding 20 mmol/m^3 similarly stretched northward into the Makarov Basin (Figure 3b). Rough boundary lines were drawn to mark the apparent transition (or front) from higher to lower Pacific water fractions and silicate concentrations (blue dots in each panel). In contrast, the NO distribution along this isohaline (Figure 3c) indicated that higher NO values (>400 mmol/m^3) were restricted to the Canada Basin side of the Mendeleyev Ridge, farther south than the front implied by the Pacific water and silicate distributions. This latter front was marked as a red, dashed line on the panels of Figure 3, and its southernmost extent was located in the central ESS, at ~165°E.

The DH distribution (Figure 3d) also indicated a front that separated regions of elevated DH that extended over the Canada Basin/Beaufort Gyre from regions of depressed DH that extended over the Eurasian and Makarov Basins. This transition in DH also marks a front that is roughly located between the Pacific/silicate front and the NO front and is characterized by a denser concentration of isolines of DH in Figure 3d.

4. Discussion

4.1. Using NO to Identify the Atlantic/Pacific Front

As indicated in Figure 3, there was a substantial change in NO within the upper halocline ($32 \leq S \leq 33.5$) between the 165 and 175°E longitude lines in the ESS, though there was no obvious difference in silicate. Similarly, abrupt declines in the NO values were observed at the northern ends of both GEOTRACES Legs (Figure 2). We associate the higher NO values with halocline waters originating from the Chukchi Sea (i.e., Pacific halocline waters), whereas lower NO values were associated with an ESS origin (i.e., Atlantic halocline waters).

Semiletov et al. (2005) has previously described the ESS as a convergence zone for Atlantic waters circulating eastward along the Siberian continental slope and Pacific waters spreading westward from the Chukchi shelf and slope. More recently, Nishino et al. (2013) suggested that an expansion of the Beaufort Gyre resulted in a westward extension of Pacific halocline waters from the Chukchi Plateau to ~180° (near the Mendeleyev Ridge) between 2002 and 2008.

We argue that during the summer of 2015, the NO distribution described the convergence of Chukchi and ESS shelf waters in the central ESS and their spread northward to ventilate the upper halocline of the deep basins via the Canadian and Siberian branches of the TPD (Alkire et al., 2007). Plots of θ (Figure 4a), O_2 (Figure 4b), NO_3^- (Figure 4c), and NO (Figure 4d) versus salinity along the ~165°E (green) and 175°E (black) transect lines occupied during the NABOS-II expedition indicate that both O_2 and NO_3^- (and consequentially NO) were consistently lower along ~165°E than ~175°E within the salinity range of the upper halocline ($32 \leq S \leq 33.5$). We suggest that this difference in NO reflects contributions of shelf waters from the East Siberian versus Chukchi Seas.

Both Western Chukchi Summer Water and Pacific Winter Water (Shimada et al., 2001, 2005) have been shown to exhibit maxima in the NO parameter, whereas Siberian shelf waters ventilating the Atlantic/eastern Arctic halocline typically exhibit lower NO values (Alkire et al., 2010; Jones & Anderson, 1986; Wilson & Wallace, 1990). The higher NO values associated with the Pacific halocline waters result from both higher NO_3^- and O_2 concentrations (Figures 2, 4, and S6). Although nutrient input and O_2 depletion result from the interaction of shelf waters with bottom sediments during transport across both the Chukchi and ESS shelves (Cooper et al., 1997; Jones & Anderson, 1986), the Pacific inflow through Bering Strait carries a higher, preformed NO_3^- concentration. Sediments on both shelves are active sites of aerobic and anaerobic respiration of OM that depletes O_2 (or NO_3^-, in the case of denitrification) and releases

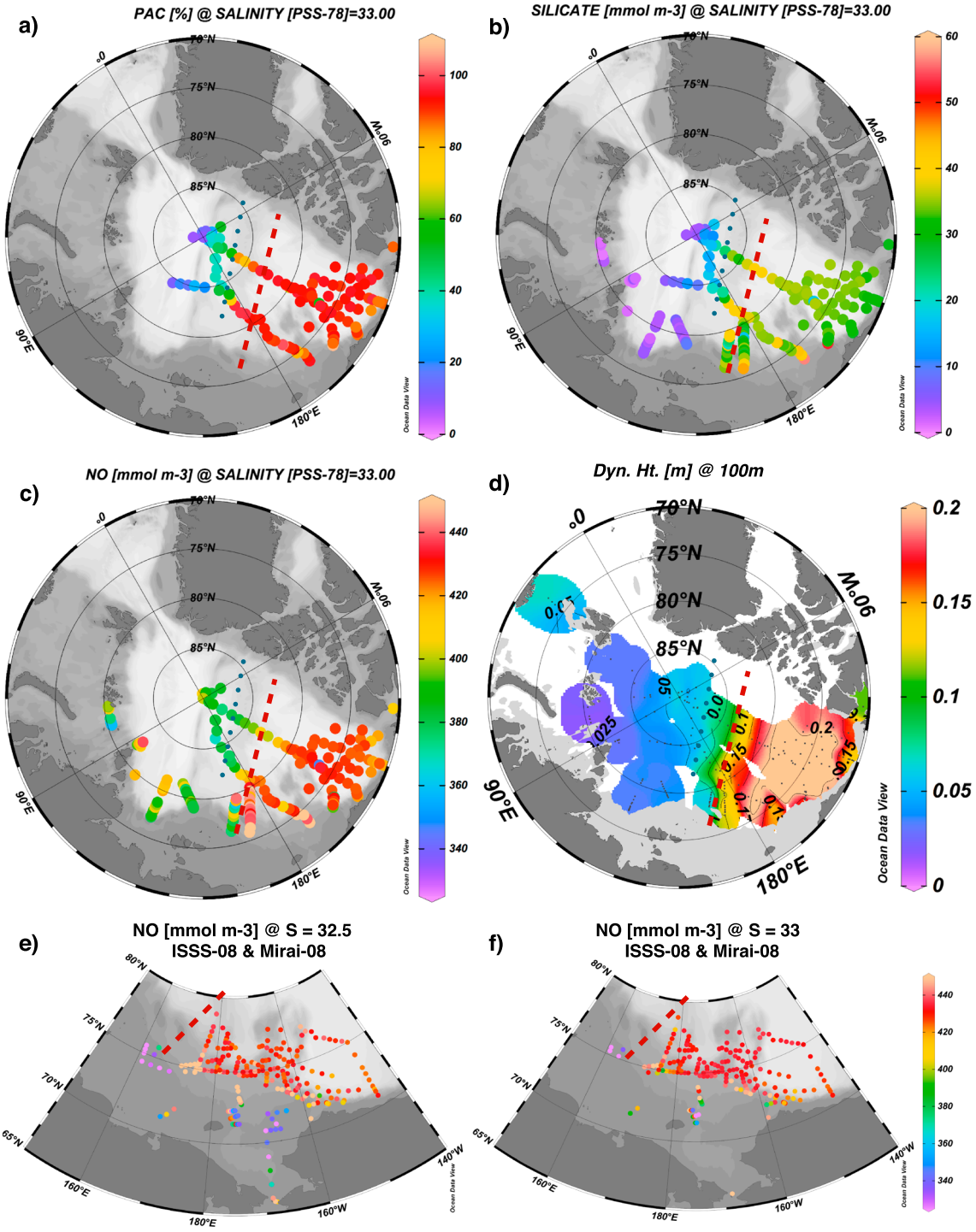

Figure 3. Plots of (a) Pacific water fraction, (b) silicate concentration, and (c) NO on the S = 33 isohaline during summer 2015 and (d) gridded product of the dynamic height at 100 m, calculated relative to a prescribed level of no motion at 250 m. Plots of NO on the (e) S = 32.5 and (f) S = 33 isohalines from data collected during the International Siberian Shelf Study-08 (ISSS-08) and Mirai 2008 expeditions. The dotted blues lines mark the transition from higher to lower Pacific water fractions. The dashed red lines mark a similar transition in NO values. Note that Pacific water fractions were calculated using only NO_3^- and PO_4^{3-} concentrations; details provided in Text S2 of the supporting information. Panels created using Ocean Data View Software (Schlitzer, 2006).

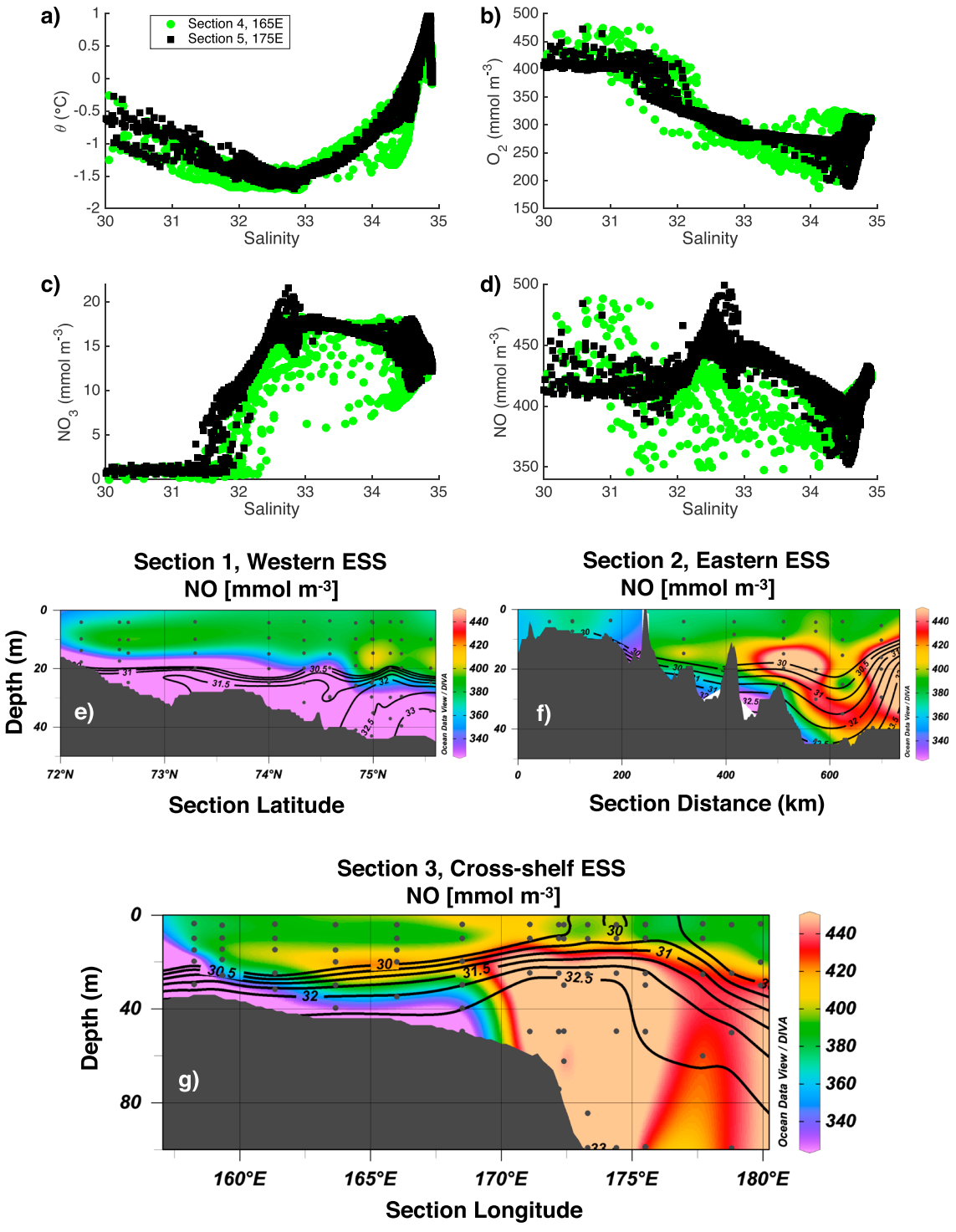

Figure 4. Plots of salinity versus (a) potential temperature (θ), (b) O_2, (c) NO_3, and (d) NO along sections 4 (green circles) and 5 (black squares) occupied during the 2015 Nansen and Amundsen Basin Observation System II (NABOS-II) expedition (see Figure 1 for section locations). Vertical sections of NO plotted from data collected during International Siberian Shelf Study-08 (ISSS-08). Sections (e) 1 and (f) 2 were located in the Western and Eastern East Siberian Sea (ESS), respectively, whereas (g) section 3 cut across the ESS shelf from west to east (see Figure 1b for section locations). Bottom topography from IBCAO (version 3) 90- × 30-s bathymetry. Panels created using Ocean Data View Software (Schlitzer, 2006).

inorganic nutrients back to the water column (Devol et al., 1997; Nitishinsky et al., 2007). However, Siberian shelves do not receive a substantial, preformed nutrient inflow from the Pacific; instead, waters are composed of Atlantic seawater and river runoff that are characterized by somewhat lower nutrient concentrations (Holmes et al., 2012; McClelland et al., 2011; Torres-Valdes et al., 2013). Furthermore, Siberian shelves receive a substantial input of allochthonous OM in both dissolved and particulate forms; the remineralization of this additional source of OM to shelf sediments may be responsible for the reduced O_2 concentrations observed on the western ESS shelf. In addition, terrigenous sources of OM are relatively nitrogen-poor compared to OM derived from marine productivity (Lobbes et al., 2000); this factor may also contribute to the lower NO values observed on the western ESS shelf.

Previous work conducted as part of the ISSS-08 (Anderson et al., 2013) confirms a significant difference in NO between the western and eastern regions of the ESS shelf (Figures 4e–4g). For example, bottom waters with salinities >32.5 were characterized by lower O_2 (Figure S4) and NO (Figure 4e) in the western shelf region compared to the eastern shelf region (Figure 4f), despite similar silicate concentrations (Figure S4). In fact, a zonal section across the shelf break (Figures 4g and S5) indicates the convergence of low NO waters from the west with higher NO waters from the east between longitudes of 165 and 170°E, quite similar to the general location of the front observed in the NABOS-II data. Maps of NO on $S = 32.5$ and $S = 33$ isohaline surfaces (Figures 3e and 3f) also show that the shelf break and slope of the western ESS exhibited lower NO values compared to those observed farther east; thus, lower NO waters from the western ESS may have also been advected off the shelf to the deep basin during summer 2008, but the available data coverage was not sufficient to capture it.

4.2. Implications for Identifying and Quantifying Pacific Water Contributions

The results of this study suggest that ESS waters ventilated the upper halocline of the Makarov Basin/central Arctic, whereas the Chukchi/Pacific waters ventilated the Canada Basin. These interpretations support conclusions by Kipp et al. (2018) that utilized measurements of radium and sea ice back trajectories to argue that the ESS was the source of surface waters to the central Arctic region during summer 2015. Thus, it appears that the circulation of surface and UHWs were coupled via their transport within the TPD in 2015. Alkire et al. (2007) has argued that the circulation of surface and UHWs in the central Arctic may not necessarily be coupled. Whether the results of this study indicate a significant change in circulation due to, for example, the extended open water period over the ESS during autumn and winter (Anderson et al., 2013; Nishino et al., 2013), or is related to the phase of the Arctic Oscillation requires further study. However, we note that both 2008 and 2015 were classified as positive (cyclonic) years in terms of the Arctic Oscillation (Figure S8); thus, the restriction of Pacific water to the Canada Basin would be expected based on idealized circulation regimes (Morison et al., 2012).

Previous measurements conducted in the central Arctic Ocean during spring 2007 and 2008 also indicated that lower NO waters ventilated the halocline of the Makarov Basin and it was speculated that these waters originated on the Siberian shelves (Alkire et al., 2010). However, Pacific water fractions and silicate concentrations measured from the central Arctic Ocean during April and August of 2015 via the NPEO and GEOTRACES expeditions, respectively, suggest that Pacific waters were present as far north as the Pole (Figures 2 and 3). How do we explain this discrepancy?

Relatively high silicate concentrations (>20 mmol/m^3) were observed over a fairly wide salinity range, $32 \leq S \leq 33.5$, and extended as far north as ~85°N along both the West and East Legs of the GEOTRACES cruise. Typically, higher silicate concentrations would be interpreted as a sign of Pacific water influence, but we suggest they originated from the ESS. Anderson et al. (2013) suggested the ESS as a potential source region of UHWs ventilating the deep basins of the Arctic Ocean and attributed the formation of this new water source to the delay in ice formation over the ESS shelf starting in 2004. Using data collected primarily south of 76°N and between 150 and 170°E, they observed clear geochemical signatures of OM remineralization in shelf bottom waters; however, these waters are typically not saline enough to ventilate the upper halocline. But, waters exhibiting similar geochemical signatures as those on the shelf (i.e., higher silicate concentrations, lower O_2 concentrations, and low pH) and of sufficiently high salinities ($S \geq 32.5$) to ventilate the halocline were observed at the ESS shelf break (e.g., see Figures 3e and 3f and 4e–4g). Anderson et al. (2013) suggested the modification of Atlantic waters upwelled onto the shelf break as one possible mechanism to produce these halocline waters, noting that similar observations of high silicate concentrations

extending over a wider salinity range than is typical of Pacific Winter Waters (S~33.1) was previously reported east of the Chukchi Plateau by Woodgate et al. (2005). They further suggested that these halocline waters originated on the western and/or eastern ESS shelves, likely formed during winter months due to enhanced brine production, and subsequently progressed northeastward with the eastward flowing circulation. They even suggested a specific region (73°N, 155°E)—in the western ESS—where the lowest O_2 and pH values were observed, as a potential source region for the shelf waters contributing to the halocline.

Pacific water fractions ranging between 20 and 40% were estimated from NO_3^- and PO_4^{3-} measurements collected north of 85°N in the Makarov Basin (Figure 3a); however, previous studies (Alkire et al., 2015; Bauch et al., 2011; Nitishinsky et al., 2007) have indicated that sedimentary denitrification on the Laptev and ESS shelves are likely to impact these shelf waters and complicate the quantitative calculation of Pacific water contributions to seawater samples using nutrient relationships. Typically, the methods utilized to estimate Pacific water contributions are associated with an uncertainty of ±13% (Alkire et al., 2015); however, a comparison of the fronts drawn in the panels of Figure 3 suggests that the uncertainties associated with these methods may be ≥40%.

5. Conclusions

The observations presented in this study suggest that a front separating UHW contributions from the Atlantic and Pacific was roughly aligned with the origin of the TPD in the central ESS during summer 2015. This front was recognized primarily due to significant contrasts in the NO parameter, since the western shelf waters exhibited much lower NO compared to those observed farther east (Figures 2 and 3). The results of this study support previous assertions that UHWs in the deep basins of the Arctic are at least partially ventilated by waters originating from the ESS (Alkire et al., 2010; Anderson et al., 2013; Nishino et al., 2013).

These results also demonstrate the utility of the NO parameter for qualitative identification of important hydrographic fronts in the Arctic Ocean, such as the Atlantic/Pacific front (or perhaps more specifically, the western ESS shelf water/Chukchi shelf water front) and the influence of shelf-derived waters to the Arctic halocline. These capabilities should prove useful, since the often relied upon methods by which Pacific water has been distinguished in the Arctic Ocean (i.e., silicate maxima centered around a salinity of ~33 and/or DIN:PO_4^{3-} relationships) are no longer reliable and may not be used with confidence to identify Pacific water influence in the central Arctic. Instead, alternate tracers, such as ^{129}I (e.g., Smith et al., 1998) and the NO parameter, will need to be included in future studies to accurately identify fronts separating Pacific and Atlantic water contributions to the Arctic halocline.

Acknowledgments
Details of the various data sources used in this study are reported in Table S1. Alkire acknowledges funding from the National Science Foundation (PLR-1203146 AM003) and the National Oceanic and Atmospheric Administration (NA15OAR4310156). Any opinions, findings, and conclusions or recommendations expressed in this material are those of the author(s) and do not necessarily reflect the views of the National Science Foundation or the National Oceanic and Atmospheric Administration.

References

Aagaard, K., Coachman, L. K., & Carmack, E. (1981). On the halocline of the Arctic Ocean. *Deep Sea Research Part A. Oceanographic Research Papers*, *28*(6), 529–545. https://doi.org/10.1016/0198-0149(81)90115-1

Alkire, M. B., Falkner, K. K., Morison, J., Collier, R. W., Guay, C. K., Desiderio, R. A., et al. (2010). Sensor-based profiles of the NO parameter in the central Arctic and southern Canada Basin: New insights regarding the cold halocline. *Deep-Sea Research Part I*, *57*(11), 1432–1443. https://doi.org/10.1016/j.dsr.2010.07.011

Alkire, M. B., Falkner, K. K., Rigor, I., Steele, M., & Morison, J. (2007). The return of Pacific waters to the upper layers of the central Arctic Ocean. *Deep-Sea Research Part I*, *54*(9), 1509–1529. https://doi.org/10.1016/j.dsr.2007.06.004

Alkire, M. B., Morison, J., & Andersen, R. (2015). Variability and trends in the meteoric water, sea-ice melt, and Pacific water contributions to the central Arctic Ocean, 2000-2013. *Journal of Geophysical Research: Oceans*, *120*, 1573–1598. https://doi.org/10.1002/2014JC010023

Alkire, M. B., Polyakov, I., Rember, R., Ashik, I. M., Ivanov, V., & Pnyushkov, A. V. (2017). Lower halocline water formation and modification, a comparison of physical and geochemical methods. *Ocean Science*, *13*(6), 983–995. https://doi.org/10.5194/os-13-983-2017

Anderson, L. G., Andersson, P. S., Björk, G., Jones, E. P., Jutterström, S., & Wåhlström, I. (2013). Source and formation of the upper halocline of the Arctic Ocean. *Journal of Geophysical Research: Oceans*, *118*, 410–421. https://doi.org/10.1029/2012JC008291

Anderson, L. G., Björk, G., Holby, O., Jutterström, S., O'Regan, C. M., Pearce, I., et al. (2017). Shelf -basin interaction along the Laptev-East Siberian Sea. *Ocean Science*, *13*(2), 349–363. https://doi.org/10.5194/os-13-349-2017

Ardyna, M., Babin, M., Gosselin, M., Devred, E., Rainville, L., & Tremblay, J.-É. (2014). Recent Arctic Ocean sea ice loss triggers novel fall phytoplankton blooms. *Geophysical Research Letters*, *41*, 6207–6212. https://doi.org/10.1002/2014GL061047

Bauch, D. R. v. d. L., Michiel, M., Andersen, N., Torres-Valdes, S., Bakker, K., & Abrahamsen, E. P. (2011). Origin of freshwater and polynya water in the Arctic Ocean halocline in summer 2007. *Progress in Oceanography*, *91*(4), 482–495. https://doi.org/10.1016/j.pocean.2011.07.017

Broecker, W. S. (1974). "NO": A conservative water mass tracer. *Earth and Planetary Science Letters*, *23*(1), 100–107. https://doi.org/10.1016/0012-821X(74)90036-3

Coachman, L. K., & Barnes, C. A. (1961). The contribution of Bering Sea water to the Arctic Ocean. *Arctic*, *14*, 147–161.

Cooper, L. W., Whitledge, T. E., Grebmeier, J. M., & Weingartner, T. (1997). The nutrient, salinity, and stable oxygen isotope composition of Bering and Chukchi Seas waters in and near the Bering Strait. *Journal of Geophysical Research*, *102*(C6), 12,563–12,573. https://doi.org/10.1029/97JC00015

Devol, A. H., Codispoti, L. A., & Christensen, J. P. (1997). Summer and winter denitrification rates in western Arctic shelf sediments. *Continental Shelf Research*, *17*(9), 1029–1050. https://doi.org/10.1016/S0278-4343(97)00003-4

Dodd, P. A., Rabe, B., Hansen, E., Falck, E., Mackensen, A., Rohling, E., et al. (2012). The freshwater composition of the Fram Strait outflow derived from a decade of tracer measurements. *Journal of Geophysical Research*, *117*, C11005. https://doi.org/10.1029/2012JC008011

Falck, E., Kattner, G., & Budéus, G. (2005). Disappearance of Pacific water in the northwestern Fram Strait. *Geopysical Research Letters*, *32*, L14619. https://doi.org/10.1029/2005GL023400

Holmes, R. M., McClelland, J. W., Peterson, B. J., Tank, S. E., Bulygina, E., Eglinton, T. I., et al. (2012). Seasonal and annual fluxes of nutrients and organic matter from large rivers to the Arctic Ocean and surrounding seas. *Estuaries and Coasts*, *35*(2), 369–382. https://doi.org/10.1007/s12237-011-9386-6

Itoh, M., Carmack, E., Shimada, K., McLaughlin, F., Nishino, S., & Zimmermann, S. (2007). Formation and spreading of Eurasian source oxygen-rich halocline water into the Canadian Basin in the Arctic Ocean. *Geophysical Research Letters*, *34*, L08603. https://doi.org/10.1029/2007GL029482

Jones, E. P., & Anderson, L. G. (1986). On the origin of the chemical properties of the Arctic Ocean halocline. *Journal of Geophysical Research*, *91*(C9), 10,759–10,767. https://doi.org/10.1029/JC091iC09p10759

Jones, E. P., Anderson, L. G., & Swift, J. H. (1998). Distribution of Atlantic and Pacific waters in the Arctic Ocean: Implications for circulation. *Geophysical Research Letters*, *25*(6), 765–768. https://doi.org/10.1029/98GL00464

Kipp, L. E., Charette, M. A., Moore, W. S., Henderson, P. B., & Rigor, I. G. (2018). Increased fluxes of shelf-derived materials to the central Arctic Ocean. *Science Advances*, *4*(1), eaao1302. https://doi.org/10.1126/sciadv.aao1302

Lobbes, J. M., Fitznar, H. P., & Kattner, G. (2000). Biogeochemical characteristics of dissolved and particulate organic matter in Russian rivers entering the Arctic Ocean. *Geochimica et Cosmochimica Acta*, *64*(17), 2973–2983. https://doi.org/10.1016/S0016-7037(00)00409-9

McClelland, J. W., Holmes, R. M., Dunton, K. H., & Macdonald, R. W. (2011). The Arctic Ocean Estuary. *Estuaries and Coasts*, *35*(2), 353–368. https://doi.org/10.1007/s12237-010-9357-3

McLaughlin, F. A., Carmack, E., & Macdonald, R. (1996). Physical and geochemical properties across the Atlantic/Pacific water mass front in the southern Canadian Basin. *Journal of Geophysical Research*, *101*(C1), 1183–1197. https://doi.org/10.1029/95JC02634

Morison, J., Kwok, R., Peralta-Ferriz, C., Alkire, M., Rigor, I., Andersen, R., & Steele, M. (2012). Changes in Arctic Ocean circulation and freshwater measure with ICESat altimetry, GRACE gravimetry, and *in situ* observations. *Nature*, *481*, 66–70. https://doi.org/10.1038/nature10705(7379)

Morison, J., Steele, M., & Andersen, R. (1998). Hydrography of the upper Arctic Ocean measured from the nuclear submarine U.S.S. Pargo. *Deep Sea Research*, *45*(1), 15–38. https://doi.org/10.1016/S0967-0637(97)00025-3

Morison, J., Steele, M., Kikuchi, T., Falkner, K., & Smethie, W. (2006). The relaxation of central Arctic Ocean hydrography to pre-1990s climatology. *Geophysical Research Letters*, *33*, L17604. https://doi.org/10.1029/2006GL026826

Morison, J. H., Aagaard, K., Falkner, K. K., Hatakeyama, K., Moritz, R., Overland, J. E., et al. (2002). North Pole environmental observatory delivers early results. *Eos, Transactions of the American Geophysical Union*, *83*(33), 357. https://doi.org/10.1029/2002EO000259

Morison, J. H., Aagaard, K., & Steele, M. (2000). Recent environmental changes in the Arctic: A review. *Arctic*, *53*(4). https://doi.org/10.14430/arctic867

Nishino, S., Itoh, M., Williams, W. J., & Semiletov, I. (2013). Shoaling of the nutricline with an increase in near-freezing temperature water in the Makarov Basin. *Journal of Geophysical Research: Oceans*, *118*, 635–649. https://doi.org/10.1029/2012JC008234

Nishino, S., Shimada, K., Itoh, M., Yamamoto-Kawai, M., & Chiba, S. (2008). East-west differences in water mass, nutrient, and chlorophyll *a* distribution in the sea ice reduction region of the western Arctic Ocean. *Journal of Geophysical Research*, *113*, C00A01. https://doi.org/10.1029/2007JC004666

Nitishinsky, M., Anderson, L. G., & Holemann, J. A. (2007). Inorganic carbon and nutrient fluxes on the Arctic Shelf. *Continental Shelf Research*, *27*(10-11), 1584–1599. https://doi.org/10.1016/j.csr.2007.01.019

Polyakov, I. V., Pnyushkov, A. V., Alkire, M. B., Ashik, I. M., Baumann, T. M., Carmack, E. C., et al. (2017). Greater role for Atlantic inflows on sea-ice loss in the Eurasian Basin of the Arctic Ocean. *Science*, *356*(6335), 285–291. https://doi.org/10.1126/science.aai8204

Rudels, B., Anderson, L. G., & Jones, E. P. (1996). Formation and evolution of the surface mixed layer and halocline of the Arctic Ocean. *Journal of Geophysical Research*, *101*(C4), 8807–8821. https://doi.org/10.1029/96JC00143

Rudels, B., Jones, P., Schauer, U., & Eriksson, P. (2004). Atlantic sources of the Arctic Ocean surface and halocline waters. *Polar Research*, *23*(2), 181–208. https://doi.org/10.1111/j.1751-8369.2004.tb00007.x

Schlitzer, R. (2006). Ocean data view. Retrieved from http://odv.awi.de

Semiletov, I., Dudarev, O., Luchin, V., Charkin, A., Shin, K.-H., & Tanaka, N. (2005). The East Siberian Sea as a transition zone between Pacific-derived waters and Arctic shelf waters. *Geophysical Research Letters*, *32*, L10614. https://doi.org/10.1029/GL022490

Shimada, K., Carmack, E. C., Hatakeyaman, K., & Takizawa, T. (2001). Varieties of shallow temperature maximum waters in the western Canadian Basin of the Arctic Ocean. *Geophysical Research Letters*, *28*(18), 3441–3444. https://doi.org/10.1029/2001GL013168

Shimada, K., Itoh, M., Nishino, S., McLaughlin, F., Carmack, E., & Proshutinsky, A. (2005). Halocline structure in the Canada Basin of the Arctic Ocean. *Geophysical Research Letters*, *32*, L03605. https://doi.org/10.1029/2004GL021358

Smith, J. N., Ellis, K. M., & Kilius, L. R. (1998). ^{129}I and ^{137}Cs tracer measurements in the Arctic Ocean. *Deep-Sea Research Part I*, *45*(6), 959–984. https://doi.org/10.1016/S0967-0637(97)00107-6

Steele, M., & Boyd, T. (1998). Retreat of the cold halocline layer in the Arctic Ocean. *Journal of Geophysical Research*, *103*(C5), 10,419–10,435. https://doi.org/10.1029/98JC00580

Steele, M., Morison, J., Ermold, W., Rigor, I., & Ortmeyer, M. (2004). Circulation of summer Pacific halocline water in the Arctic Ocean. *Journal of Geophysical Research*, *109*, C02027. https://doi.org/10.1029/2003JC002009

Taylor, J. R., Falkner, K. K., Schauer, U., & Meredith, M. (2003). Quantitative considerations of dissolved barium as a tracer in the Arctic Ocean. *Journal of Geophysical Research*, *108*(C12), 3374. https://doi.org/10.1029/2002JC001635

Torres-Valdes, S., Tsubouchi, T., Bacon, S., Naveira-Garabato, A. C., Sanders, R., McLaughlin, F. A., et al. (2013). Export of nutrients from the Arctic Ocean. *Journal of Geophysical Research: Oceans*, *118*, 1625–1644. https://doi.org/10.1002/jgrc.20063

Wilson, C., & Wallace, D. W. R. (1990). Using the nutrient ratio NO/PO as a tracer of continental shelf waters in the central Arctic Ocean. *Journal of Geophysical Research*, *95*(C12), 22,193–22,208. https://doi.org/10.1029/JC095iC12p22193

Woodgate, R. A., Aagaard, K., Swift, J. H., Falkner, K. K., & Smethie, W. M. Jr. (2005). Pacific ventilation of the Arctic Ocean's lower halocline by upwelling and diapycnal mixing over the continental margin. *Geophysical Research Letters*, *32*, L18609. https://doi.org/10.1029/2005GL023999

Yamamoto-Kawai, M., McLaughlin, F. A., Carmack, E. C., Nishino, S., & Shimada, K. (2008). Freshwater budgets of the Canada Basin, Arctic Ocean, from salinity, $\delta^{18}O$, and nutrients. *Journal of Geophysical Research*, *113*, C01007. https://doi.org/10.1029/2006JC003858